

Analyst

Accepted Manuscript



This is an *Accepted Manuscript*, which has been through the Royal Society of Chemistry peer review process and has been accepted for publication.

Accepted Manuscripts are published online shortly after acceptance, before technical editing, formatting and proof reading. Using this free service, authors can make their results available to the community, in citable form, before we publish the edited article. We will replace this *Accepted Manuscript* with the edited and formatted *Advance Article* as soon as it is available.

You can find more information about *Accepted Manuscripts* in the [Information for Authors](#).

Please note that technical editing may introduce minor changes to the text and/or graphics, which may alter content. The journal's standard [Terms & Conditions](#) and the [Ethical guidelines](#) still apply. In no event shall the Royal Society of Chemistry be held responsible for any errors or omissions in this *Accepted Manuscript* or any consequences arising from the use of any information it contains.

1
2
3
4 **Multicolor ELISA based on alkaline phosphatase-triggered**
5
6
7 **growth of Au nanorods**
8
9

10 Yanyan Li,^a Xiaoming Ma,^a Zhengming Xu,^a Meihua Liu,^b Zhenyu Lin,^{a*} Bin Qiu,^a

11
12
13 Longhua Guo^{a*} and Guonan Chen^a
14
15

16
17 ^a Institute of Nanomedicine and Nanobiosensing; The Key Lab of Analysis and Detection
18
19
20 Technology for Food Safety of the MOE and Fujian Province; College of Chemistry,
21
22
23 Fuzhou University, Fuzhou, 350116, China.
24

25 ^b Fuqing Branch of Fujian Normal University, Fuqing, Fujian 350300, China
26
27

28 * To whom correspondence should be addressed. E-mail: guolh@fzu.edu.cn (Longhua
29
30
31 Guo); zylin@fzu.edu.cn (Zhenyu Lin); Tel: +86-591-22866164; Fax: +86-591-22866135
32
33
34
35
36
37
38
39
40
41
42
43
44
45
46
47
48
49
50
51
52
53
54
55
56
57
58
59
60

ABSTRACT

Seed-mediated synthesis of gold nanorods (AuNRs) has been widely used for diverse applications in the past decade. In this work, this synthetic process is demonstrated for multicolor biosensing for the first time. Our investigation reveals that ascorbic acid acts as a key factor to mediate the growth of AuNRs. This phenomenon is incorporated into the alkaline phosphatase (ALP)- Enzyme-linked immunosorbent assay (ELISA) system based on the fact that ALP can catalyze the conversion of ascorbic acid-phosphate into ascorbic acid with high efficiency. This allows us to develop a multicolor ELISA approach for sensitive detection of disease biomarkers with the naked eye. We show the proof-of-concept multicolor ELISA for the detection of prostate-specific antigen (PSA) in human serum. The results show that different colors are presented in response to different concentrations of PSA, and a detection limit of 3×10^{-15} g/mL in human serum was achieved. The proposed multicolor ELISA could be a good supplementary to conventional ELISA for POC diagnostics.

Keywords: Au nanorod; ELISA; visual inspection; alkaline phosphatase; clinical diagnosis

INTRODUCTION

Colorimetric sensors have attracted broad interests to both the academic and industrial communities due to their simplicity and affordability.¹⁻⁵ Normally, colorimetric sensors can be detected with a portable UV-Vis spectrometer or even inspected with the naked eye.⁶⁻⁷ Therefore, colorimetric sensors are extremely suitable for those applications that expensive and/or bulky equipments are not applicable, for example, point-of-care testing (POCT) and *in situ* environmental/food inspection.⁸⁻¹⁰ Although colorimetric sensors were extensively explored in the past decades, great challenges still exist to turn these laboratory available sensors into real applications. An ideal colorimetric sensor which is feasible for real applications should at least satisfy the following conditions: 1) High sensitivity. The sensitivity of the sensor should be high enough, when compared with other sensors such as fluorescent- and electrochemical- based sensors. 2) Wide applicability. The sensor should be specific to the target while the sensing strategy should be widely applicable to a number of analytes so that it is easier to be commercialized. 3) Naked-eye (semi)quantitative assay. Visual inspection of the analytes with the naked eye is the unique advantage of colorimetric sensors. However, the accuracy of the sensor should be improved so that naked-eye inspection can not only be used for qualitative assays, but also used for (semi)quantitative assays. Recently, we demonstrated that colorimetric sensor based on the oriented aggregation of Au nanoparticles (AuNPs) can improve the sensitivity effectively, which is comparable to fluorescent based approaches.¹¹ However, the color response of the sensor was still not enough for

1
2
3
4 (semi)quantitative naked-eye inspection, thus a spectral meter was still necessary to be
5
6
7 used for the detection. Herein, we demonstrated that colorimetric sensors based on the
8
9
10 combination of conventional Enzyme-linked immunosorbent assay (ELISA) and
11
12 enzyme-triggered growth of Au nanorods (AuNRs) could almost satisfy all the above
13
14 mentioned criteria.

15
16
17 ELISA is a widely used immunoassay method based on biocatalytic property of an
18
19 enzyme and the antigen antibody recognition.¹²⁻¹³ Due to the extremely high biocatalytic
20
21 ability of the labeled enzyme, ELISA methods are usually highly sensitive; while the
22
23 antigen-antibody recognition ensures the specificity of the approach. In addition,
24
25 thousands of antibodies have been commercialized, so that ELISA can detect a broad
26
27 range of targets. For example, ELISA has been extensively used in many fields such as
28
29 clinical diagnosis, environmental monitoring, food quality control, laboratory research,
30
31 and so on.¹⁴⁻¹⁹ In conventional colorimetric ELISA, a signal is generated by the
32
33 conversion of the enzyme substrate into a colored molecule, and the intensity of the color
34
35 of the solution is increased with the concentration of the target. This single-color intensity
36
37 variation is insensitive to human eyes, thus naked-eye inspection can be only used for
38
39 qualitative detection of the target, while a microplate reader should be used for
40
41 quantitative determination of the concentration of the analytes. However, the costly and
42
43 bulky microplate reader prevents its utility for POC testing.²⁰⁻²¹

44
45
46 Recently, the unique optical properties of the noble metal nanoparticles were
47
48 incorporated into conventional ELISA to develop a new immunoassay method called
49
50
51
52
53
54
55
56
57
58
59
60

1
2
3
4 plasmonic ELISA.²²⁻²³ The results showed that plasmonic ELISA presented enhanced
5
6 color display compared with conventional colorimetric ELISA so that it can be utilized
7
8 for visual detection of the analytes with the naked eye. For example, Stevens and
9
10 coworkers reported the first plasmonic ELISA for ultrasensitive detection of prostate
11
12 specific antigen (PSA) and HIV-1 capsid antigen p24.²⁴⁻²⁵ The absence and presence of
13
14 target molecules induced the growth of spherical gold nanoparticles (AuNPs) and
15
16 ill-defined gold nanoparticle aggregates, respectively. As a consequence, the solution
17
18 color transferred from red to blue with the increase of targets concentration. Recently, the
19
20 same strategy was utilized for the detection of HIV-1 protein gp120 at ultralow
21
22 concentrations.²⁶ Researchers from other groups have also explored diverse plasmonic
23
24 ELISA based on the formation of AuNPs aggregates.²⁷⁻²⁸ Noting that all these plasmonic
25
26 ELISA approaches showed red to blue transformation in response to different
27
28 concentration of analytes. These dual-color responses are still not accurate for
29
30 (semi)quantitative detection of the analytes with the naked eye.
31
32
33
34
35
36
37
38
39
40

41
42 In this work, we demonstrate a novel strategy for the fabrication of plasmonic
43
44 ELISA based on enzyme-triggered growth of AuNRs. Our method is developed based on
45
46 the alkaline phosphatase (ALP) ELISA system. ALP is a hydrolytic enzyme that plays a
47
48 crucial role in the cell signaling pathways.²⁹ It is responsible for removing phosphate
49
50 groups from many types of molecules.³⁰⁻³¹ In our sensing strategy, ALP is used for the
51
52 removal of a phosphate group from ascorbic acid-phosphate to yield the ascorbic acid to
53
54 trigger the growth of AuNRs.³²⁻³³ The presence of different amount of ascorbic acid leads
55
56
57
58
59
60

1
2
3
4 to the formation of AuNRs with different sizes and aspect ratios. Therefore, the proposed
5
6 plasmonic ELISA shows vivid color responses to a varied concentration of target
7
8 molecules.
9

10 11 12 **EXPERIMENTAL SECTION**

13
14 **Materials and instrumentations.** Cetyltrimethylammonium bromide (CTAB, 99%),
15
16 sodium borohydride, ascorbic acid-phosphate, gold (III) chloride trihydrate
17
18 (HAuCl₄·3H₂O), Tween-20, bovine serum albumin (BSA), and the PSA (human) ELISA
19
20 kit were purchased from Sigma-Aldrich. Tris (hydroxymethyl) aminomethane (Tris),
21
22 silver nitrate and ascorbic acid were purchased from Aladdin. Phosphate buffer (PBS)
23
24 was purchased from ding guo in China. The absorbance of AuNRs solutions in 96-well
25
26 plates were collected by a Microplate Reader (Thermo). The photographs of all colored
27
28 solutions were taken by a digital camera (Canon EOS 600D with EF 100mm f/2.8L IS
29
30 USM). All solutions were prepared with double-deionized water.
31
32
33
34
35
36
37
38

39 **Preparation of the AuNP seed solution.** The AuNP seed was synthesized according
40
41 to a reported literature.³⁴ Briefly, CTAB solution (5 mL, 0.20 M) was mixed with HAuCl₄
42
43 (5.0 mL, 0.50 mM) at room temperature. The mixture was vigorously stirred for 5 min.
44
45 Then, 0.60 mL of ice-cold 10 mM NaBH₄ was rapidly injected into the mixture. The
46
47 solution gradually changed into brownish yellow, indicating the formation of AuNP seed.
48
49 The seed solution was vigorous stirring for 2 min, then it was kept at 25 °C and should be
50
51 used within 2 h.
52
53
54
55
56

57 **Procedures for ascorbic acid sensing.** Ascorbic acids (0-15 μL, 0.01M) were added
58
59
60

1
2
3
4 to a mixture solution containing CTAB (125 μL , 0.2 M), AgNO_3 (1.5 μL , 0.01 M), and
5
6 HAuCl_4 (12.5 μL , 10 mM). The total volume of the solution was adjusted to 240 μL with
7
8 double-deionized water. Then, 10 μL of the seed solution was added to the above solution
9
10 to trigger the growth of AuNRs. The resulting solutions were incubated at room
11
12 temperature for 1 h. The photograph was taken with a digital camera, and the
13
14 corresponding UV–vis absorption was collected by a Microplate Reader.
15
16
17
18
19

20 **Procedures for visual detection of ALP-conjugated antibody.** ALP-conjugated
21
22 antibody solution obtained from the ELISA kit was diluted with 1 mM Tris-HCl buffer
23
24 (pH7.4) for 2500 folds before use. 10-70 μL of the diluted ALP-conjugated antibody
25
26 solution was then mixed with 50 μL of ascorbic acid-phosphate (20 mM). The mixture
27
28 solution was incubated at 37 $^\circ\text{C}$ for 1 h. After that, a mixture solution containing CTAB
29
30 (125 μL , 0.2 M), AgNO_3 (1.5 μL , 0.01 M), HAuCl_4 (12.5 μL , 10 mM) was added. The
31
32 total volume of the solution was adjusted to 240 μL with double-deionized water. Then
33
34 10 μL of the seed solution was added. The mixture solution was incubated for 1 h at room
35
36 temperature. The absorbance of the AuNRs solution was recorded by a plate reader and
37
38 corresponding photograph was taken by a digital camera.
39
40
41
42
43
44
45
46

47 **Plasmonic ELISA for visual detection of PSA.** Reagents obtained from a
48
49 commercial PSA (human) ELISA kit (Sigma-Aldrich) were used for the plasmonic
50
51 ELISA. Procedures for capture the PSA and ALP-conjugated PSA antibody were
52
53 followed by the instruction manual of the kit. Briefly, the primary antibody (4 $\mu\text{g}/\text{mL}$) in
54
55 bicarbonate buffer (100 mM, pH 9.6) was added into the wells of the microplate and
56
57
58
59
60

1
2
3
4 incubated at 4 °C overnight. After rinsing with PBST for 3 runs, 5% BSA in PBS (pH 7.4)
5
6 was added into each well as a blocking agent. Then, PSA (spiked in whole human serum)
7
8 was added at concentrations ranging from 10^{-3} to 200 pg/mL, respectively, and the
9
10 serum-only solution was set as a control. The plate was kept at 37 °C for 1 h and washed
11
12 with PBST for 3 runs. Then, 100 μ L of ALP-conjugated antibody (0.5 μ g/mL) solution
13
14 was added into each well, and incubated for 30 min. 200 μ L of PBST was added into each
15
16 well and rinsed for 3 runs. Next, 50 μ L of ascorbic acid-phosphate (20 mM) was added.
17
18 The solution was incubated at 37 °C for 1 h. Then 20 μ L of the solution was mixed with
19
20 the AuNRs growth solution containing CTAB (125 μ L, 0.2 M), AgNO₃ (1.5 μ L, 0.01 M),
21
22 and HAuCl₄ (12.5 μ L, 10 mM). The total volume of the solution was adjusted to 240 μ L
23
24 with double-deionized water. Finally, 10 μ L of the seed solution was added to trigger the
25
26 growth of AuNRs. The mixture solution was incubated for the other 1 h at room
27
28 temperature. The absorbance of the AuNRs solution was recorded and corresponding
29
30 photograph was taken.
31
32
33
34
35
36
37
38
39
40
41
42

43 RESULTS AND DISCUSSION

44
45
46 Figure 1 shows the general principle of the proposed plasmonic ELISA for the
47
48 detection of the target molecule. A widely used, commercially available ALP-ELISA
49
50 system was employed in our detection scheme. ALP is conjugated with a detection
51
52 antibody. The amount of ALP is proportional to the concentration of the target molecules
53
54 due to the sandwich-format immunoreaction. Hitherto, many enzymatic reaction
55
56
57
58
59
60

substrates have been reported for ALP-ELISA system to generate colorimetric or chemiluminescent signals.³⁵⁻³⁷ Herein, ascorbic acid-phosphate was selected as the enzymatic reaction substrate. ALP can efficiently remove a phosphate group from ascorbic acid-phosphate to produce ascorbic acid.^{28, 38-39} The obtained ascorbic acid induces the formation of AuNRs in the presence of growth solution. As it is shown in figure 1, in the absence of the target, there is no ascorbic acid generated in the solution. In this case, the ascorbic acid-phosphate in the reaction solution would reduce Au (III) to Au (I), and the solution is colorless. In the presence of the target, the conjugated ALP can catalyze the dephosphorylation of ascorbic acid-phosphate to produce ascorbic acid. Ascorbic acid can further reduce Au(I) to Au(0). In the presence of AuNP seeds and surfactant (e.g. CTAB), the reduced Au(0) would then deposit on the surface of AuNP seeds to initial the growth of AuNRs. Corresponding growth mechanism has been extensively investigated in seed-mediated synthesis of AuNRs.^{32, 40}

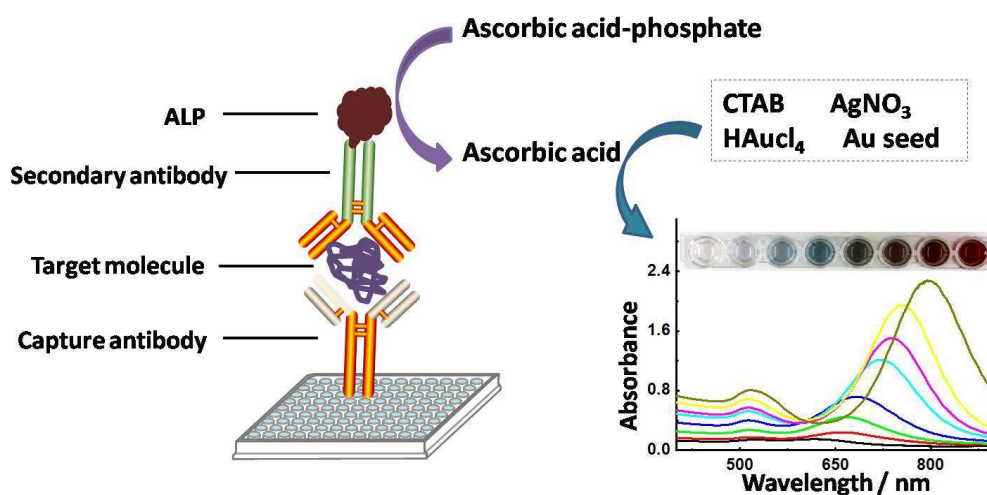


Figure 1 Schematic diagram of the plasmonic ELISA based on target-guided growth of

AuNRs

1
2
3
4
5
6
7
8
9
10
11
12
13
14
15
16
17
18
19
20
21
22
23
24
25
26
27
28
29
30
31
32
33
34
35
36
37
38
39
40
41
42
43
44
45
46
47
48
49
50
51
52
53
54
55
56
57
58
59
60

First of all, the impact of the concentration of ascorbic acid on the growth of AuNRs was investigated (Figure 2). Different concentrations of ascorbic acids were added to a growth solution containing AuNP seeds, CTAB, AgNO₃, and HAuCl₄. Noting that the formula of this growth solution was directly adopted from a literature for seed-mediated synthesis of AuNRs.³² This means that the procedures for the preparation of AuNP seeds, the concentrations of CTAB, AgNO₃, and HAuCl₄ are all followed by the instruction of the previous literature, and we didn't optimize these conditions. The resulting solutions were allowed to incubate at room temperature for 1h. It can be clearly seen from Figure 2a that the solution shows adsorption at ~400 nm, which corresponds to the extinction peak of HAuCl₄, and the solution color is yellow (see Figure 2b). After the addition of ascorbic acid, the intensity of the yellow solution decreased rapidly and then turned into colorless in the presence of 0.40 mM ascorbic acid. No obvious peak is observed at the wavelength larger than 500 nm, indicating that the AuNP seeds were not grown in this process. Therefore, we inferred that in a low concentration of ascorbic acids, the amount of ascorbic acids were not enough to reduce Au(III) to Au(0), but to Au(I). The colorless solution (Figure 2b, sample number 5) indicates the completely reducing of Au(III) into Au(I) because Au(I) (in the form of AuBr₂⁻) is colorless.⁴¹ A step further to increase the amount of ascorbic acids induced the formation of new absorption peaks at 500 nm to 800 nm, indicating the formation of AuNRs (Figure 2b, sample number 6-10). It was

observed that the intensities as well as the peak wavelength of the longitudinal peaks of AuNRs increased with the added amount of ascorbic acids. As a result, the color of these solutions changed vividly as well. These results strongly indicated that the amount of ascorbic acid played an important role in tuning the growth of AuNRs.

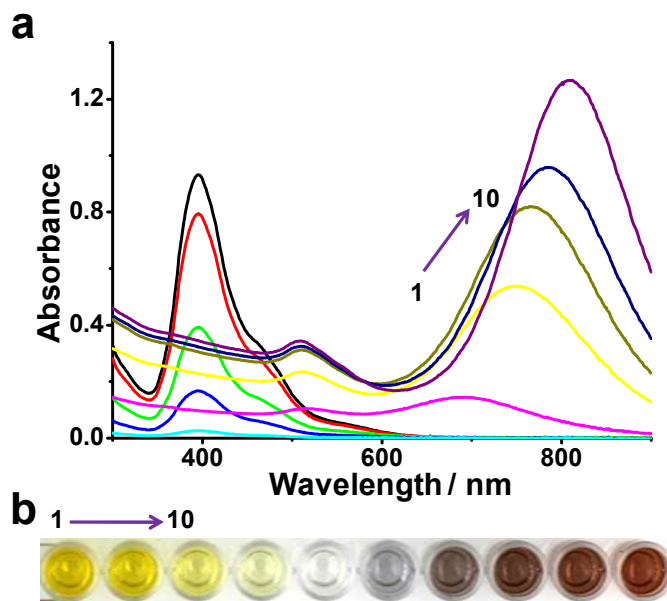
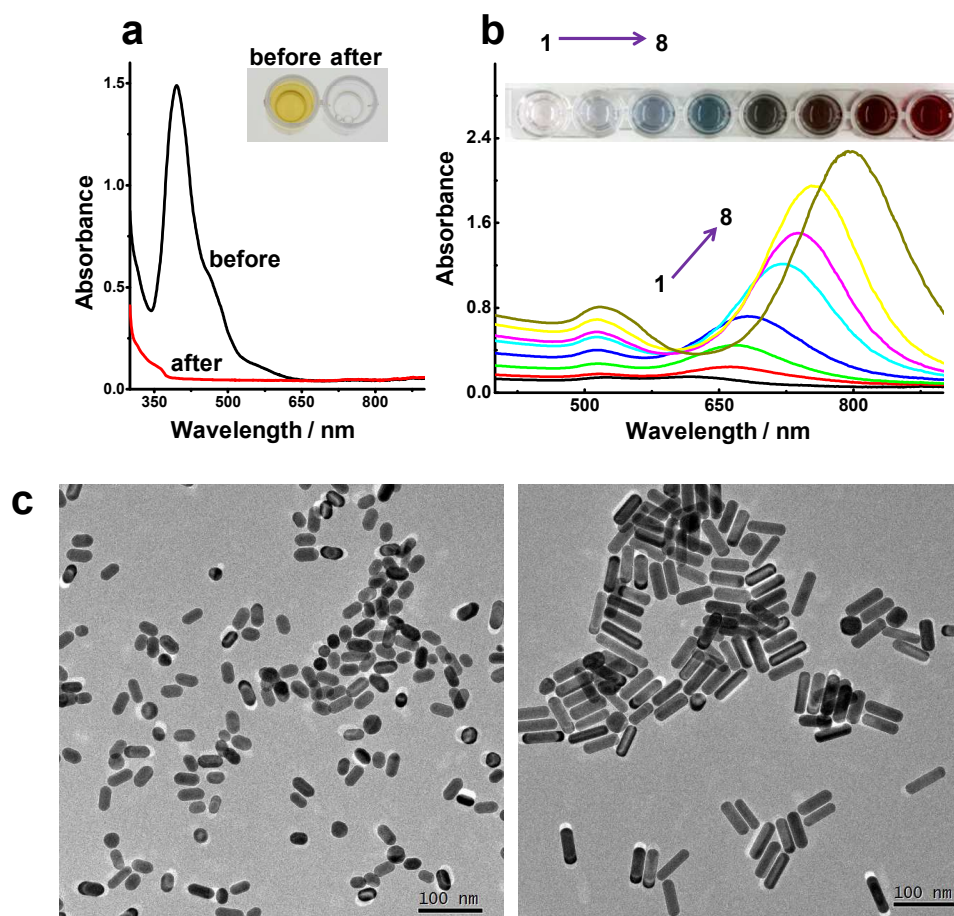


Figure 2 UV-vis spectra (a) and the corresponding photographs (b) of AuNR solutions grown with different concentrations of ascorbic acid. Concentrations of ascorbic acid for sample number 1 to 10 were 0, 0.2, 0.28, 0.36, 0.40, 0.44, 0.48, 0.52, 0.56, 0.60 mM, respectively.

Next, we investigated the growth of AuNRs based on ALP triggered conversion of ascorbic acid-phosphate to ascorbic acids (Figure 3). Figure 3a shows the extinction spectra and corresponding photographs of the growth solution before and after the addition of an excess amount of ascorbic acid-phosphate. It can be observed that the addition of ascorbic acid-phosphate into the growth solution changed the solution color from yellow to colorless. The results indicated that ascorbic acid-phosphate can also

1
2
3
4 reduce the Au(III) to Au(I). However, it cannot trigger the growth of AuNRs because no
5
6 extinction peaks are observed in the wavelength range of 500 to 800 nm even after the
7
8 addition of an excess amount of ascorbic acid-phosphate (the red curve in Figure 3a).
9
10 Therefore, the introduction of ALP to convert ascorbic acid-phosphate to ascorbic acid is
11
12
13
14
15 a necessary precondition to trigger the growth of AuNRs.
16
17



18
19
20
21
22
23
24
25
26
27
28
29
30
31
32
33
34
35
36
37
38
39
40
41
42
43
44
45
46
47
48 **Figure 3** Visual detection of ALP-antibody conjugates with the proposed plasmonic ELISA. (a)
49 UV-vis spectra and corresponding photographs of the AuNR growth solutions before and after
50 the addition of an excess amount of ascorbic acid-phosphate (50 μ L 20 mM) ; (b) UV-vis
51
52 spectra and corresponding photographs of the AuNRs growth solution after the addition of
53
54 different amount of ALP-antibody conjugates. The original solution of ALP-antibody
55
56
57
58
59
60

1
2
3
4 conjugates in the ELISA kit was diluted for 2500 times with 1 mM Tris-HCl buffer (pH 7.4). The
5 amount of diluted ALP-antibody conjugates added in sample 1 to 8 was 0, 10, 20, 30, 40, 50,
6 60, 70 μL , respectively; (c) typical TEM images corresponding to sample number 3 (left) and 8
7 (right).
8
9
10

11
12
13 In commercial available ELISA kits, ALP is presented in the form of ALP-antibody
14 conjugates. Therefore, herein we showed the effect of the concentration of ALP-antibody
15 conjugates to the growth of AuNRs (Figure 3b). ALP-antibody conjugate with various
16 concentrations were mixed with ascorbic acid-phosphate (20 mM), then the mixture was
17 incubated at 37 $^{\circ}\text{C}$ for 1 h to produce various amounts of ascorbic acids. Each of the
18 resulting solution (50 μL) was then mixed with a growth solution (200 μL) containing
19 AuNP seeds, CTAB, AgNO_3 , and HAuCl_4 . The inset in Figure 3b shows that the solution
20 color turned from colorless to purple, blue, brownish, and reddish brown in response to a
21 varied amount of ALP-antibody conjugates. The extinction spectra shown in Figure 3b
22 shows significant red-shift of the longitudinal peaks of AuNRs when increasing the
23 concentration of ALP-antibody conjugates. These results indicated that the aspect ratios
24 of AuNRs were increased with the added amount of ALP-antibody conjugates. The TEM
25 images shown in Figure 3c also support this conclusion. The close relationship between
26 the solution color (or extinction spectra) and the concentration of ALP-antibody
27 conjugates strongly indicated the feasibility of the proposed approach for visual detection
28 of ALP-antibody conjugates with the naked eye.
29
30
31
32
33
34
35
36
37
38
39
40
41
42
43
44
45
46
47
48
49
50
51
52
53
54

55
56 Finally, we demonstrated the feasibility of the proposed plasmonic ELISA for
57
58
59
60

1
2
3
4 visually detection of disease biomarkers in human serum. The detection of a cancer
5
6
7 biomarker, prostate specific antigen (PSA), was selected for a demonstration. Most of the
8
9
10 reagents for conducting the plasmonic ELISA were adopted from a commercial PSA
11
12 (human) ELISA kit (Sigma-Aldrich). Procedures for capture the PSA and
13
14 ALP-conjugated PSA antibody was followed by the instruction manual of the kit. Figure
15
16
17 4 shows the photographs (a), spectra (b) and calibration curve (c) of the proposed
18
19 plasmonic ELISA for the detection of PSA in serum. It should be pointed out that the
20
21 peak wavelength in the Y-axis means the maximum of absorbance in Fig.4b. PSA was
22
23 spiked into human serum to result in a series of samples with PSA concentrations ranging
24
25 from 10^{-3} to 200 pg/mL. The sample solution without the addition of PSA remained
26
27 colorless (see sample number 1 of Figure 4a). The solution color changed from colorless
28
29 to purple, blue, dark blue, gray, dark gray and brownish red with the increased
30
31 concentration of PSA. It should be noted that naked-eye distinguishable color was
32
33 observed in the presence of 1×10^{-15} g/mL PSA, which means that the limit of detection
34
35 (LOD) of the proposed plasmonic ELISA for the detection of PSA in human serum was
36
37 equal or lower than 1×10^{-15} g/mL. Meanwhile, significant spectral intensity and peak shift
38
39 were also observed in response to different concentration of spiked PSA (Figure 4b).
40
41
42 Good linearity between the logarithmical concentration of PSA and the corresponding
43
44 peak shifts was obtained (Figure 4c). These results strongly indicated the potential
45
46 applicability of the proposed plasmonic ELISA for the identification of disease
47
48 biomarkers at an ultralow concentration with the naked eye.
49
50
51
52
53
54
55
56
57
58
59
60

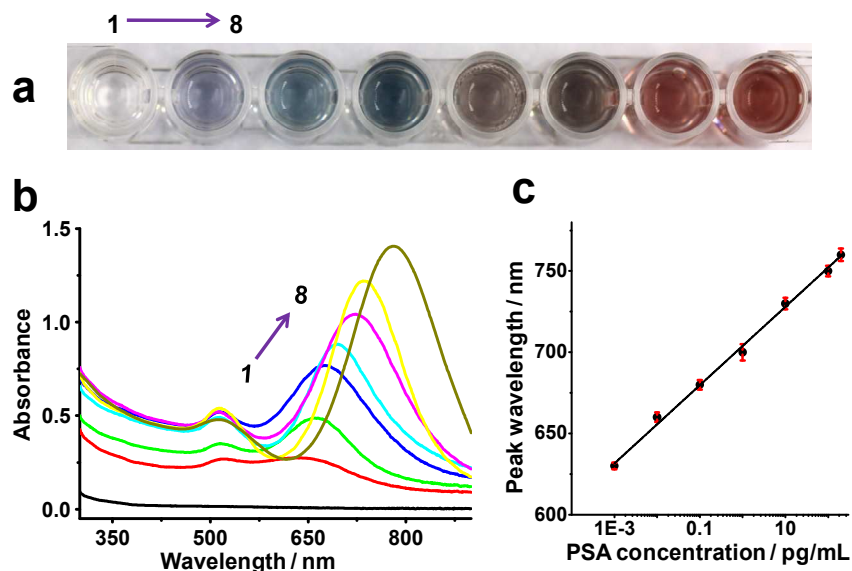


Figure 4 Photographs (a), UV-vis spectra (b), and calibration curve (c) of the proposed plasmonic ELISA for visual detection of PSA spiked in human serum. Concentrations of PSA in sample 1 to 8 are 0, 0.001, 0.01, 0.1, 1, 10, 100, and 200 pg/mL, respectively. Error bars represent standard deviation of three replicates.

Conclusions

In summary, this work demonstrated a strategy for conducting multicolor ELISA based on enzyme-triggered growth of AuNRs. ALP was used as an enzyme-label probe to specifically and efficiently catalyze the dephosphorylation of ascorbic acid-phosphate to produce ascorbic acid. The produced ascorbic acid was then used to trigger the growth of AuNRs. Our investigation revealed that different amount of ascorbic acids would produce AuNRs with different size and aspect ratios. As a result, vivid color displays were observed in response with a varied concentration of ALP. It is worth to note that ALP has been widely used in commercial ELISA kits as enzyme labels to detect a large number of

1
2
3
4 disease biomarkers. Therefore, our approach can well accommodate conventional
5
6 ALP-based ELISA to develop new multicolor ELISA methods for the detection of all
7
8 kinds of analytes. The proposed multicolor ELISA can be detected with the naked eye
9
10 with an ultrahigh sensitivity, e.g. we demonstrated the visual detection of PSA in human
11
12 serum down to 1×10^{-15} g/mL, which was much lower than current state-of-the-art ELISA
13
14 approaches detected with a sophisticated readout.
15
16
17
18
19
20
21

22 Acknowledgements

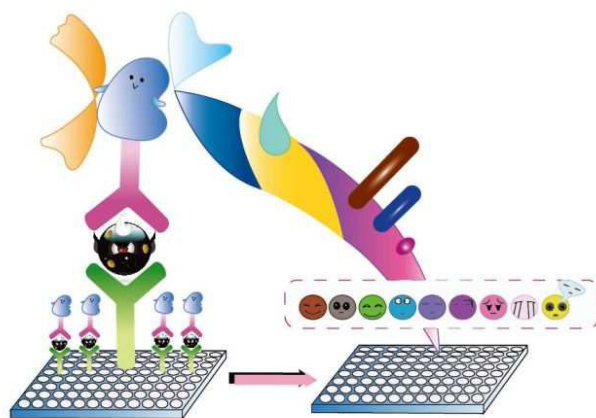
23
24 The authors gratefully acknowledge the financial support of the National Natural
25
26 Science Foundation of China (21277025, 21275031, 21375021, 21575027), the Program
27
28 for Changjiang Scholars and Innovative Research Team in University (No. IRT15R11),
29
30 and the Foundation of Fujian Educational Committee (JA12039, JA13024).
31
32
33
34
35
36
37

38 References

- 39
40
41 1. X. Zhang, J. Yin and J. Yoon, *Chem. Rev.*, 2014, 114, 4918-4959.
42 2. H. N. Kim, W. X. Ren, J. S. Kim and J. Yoon, *Chem. Soc. Rev.*, 2012, 41, 3210-3244.
43 3. L. Guo, A. R. Ferhan, H. Chen, C. Li, G. Chen, S. Hong and D. H. Kim, *Small*, 2013, 9, 234-240.
44 4. L. Guo, J. A. Jackman, H.-H. Yang, P. Chen, N.-J. Cho and D.-H. Kim, *Nano Today*, 2015, 10, 213-239.
45 5. T. Wei, T. Dong, Z. Wang, J. Bao, W. Tu and Z. Dai, *J. Am. Chem. Soc.*, 2015, 137, 8880-8883.
46 6. Q. Xu, S. Lee, Y. Cho, M. H. Kim, J. Bouffard and J. Yoon, *J. Am. Chem. Soc.*, 2013, 135,
47 17751-17754.
48 7. Z. Zhang, D. S. Kim, C.-Y. Lin, H. Zhang, A. D. Lammer, V. M. Lynch, I. Popov, O. Š. Miljanić, E. V.
49 Anslyn and J. L. Sessler, *J. Am. Chem. Soc.*, 2015, 137, 7769-7774.
50 8. C. P. Y. Chan, W. C. Mak, K. Y. Cheung, K. K. Sin, C. M. Yu, T. H. Rainer and R. Renneberg, *Annu. Rev.*
51 *Anal. Chem.*, 2013, 6, 191-211.
52 9. S. Ge, F. Liu, W. Liu, M. Yan, X. Song and J. Yu, *Chem. Commun.*, 2014, 50, 475-477.
53 10. N. R. Pollock, J. P. Rolland, S. Kumar, P. D. Beattie, S. Jain, F. Noubary, V. L. Wong, R. A. Pohlmann,
54 U. S. Ryan and G. M. Whitesides, *Science translational medicine*, 2012, 4, 152ra129-152ra129.
55
56
57
58
59
60

- 1
- 2
- 3
- 4 11. L. Guo, Y. Xu, A. R. Ferhan, G. Chen and D.-H. Kim, *J. Am. Chem. Soc.*, 2013, 135, 12338-12345.
- 5 12. J. Shen, Y. Li, H. Gu, F. Xia and X. Zuo, *Chem. Rev.*, 2014, 114, 7631-7677.
- 6 13. S. K. Vashist, E. Lam, S. Hrapovic, K. B. Male and J. H. Luong, *Chem. Rev.*, 2014, 114, 11083-11130.
- 7 14. P. L. White, C. Parr, C. Thornton and R. A. Barnes, *J. Clin. Microbiol.*, 2013, 51, 1510-1516.
- 8 15. K. Eyer, S. Stratz, P. Kuhn, S. Kuster and P. Dittrich, *Anal. Chem.*, 2013, 85, 3280-3287.
- 9 16. N. Yanagisawa and D. Dutta, *Anal. Chem.*, 2012, 84, 7029-7036.
- 10 17. A. D. Warren, S. T. Gaylord, K. C. Ngan, M. Dumont Milutinovic, G. A. Kwong, S. N. Bhatia and D. R.
11 Walt, *J. Am. Chem. Soc.*, 2014, 136, 13709-13714.
- 12 18. D. Liu, Z. Wang, A. Jin, X. Huang, X. Sun, F. Wang, Q. Yan, S. Ge, N. Xia and G. Niu, *Angew. Chem.*
13 *Int. Ed.*, 2013, 52, 14065-14069.
- 14 19. E. P. Preece, B. C. Moore, M. E. Swanson and F. J. Hardy, *Environ. Monit. Assess.*, 2015, 187, 1-10.
- 15 20. Z. Zhu, Z. Guan, D. Liu, S. Jia, J. Li, Z. Lei, S. Lin, T. Ji, Z. Tian and C. J. Yang, *Angew. Chem. Int. Ed.*,
16 2015, 54, 10448-10453.
- 17 21. J. Hu, T. Wang, J. Kim, C. Shannon and C. J. Easley, *J. Am. Chem. Soc.*, 2012, 134, 7066-7072.
- 18 22. P. D. Howes, S. Rana and M. M. Stevens, *Chem. Soc. Rev.*, 2014, 43, 3835-3853.
- 19 23. Y. Song, Y.-Y. Huang, X. Liu, X. Zhang, M. Ferrari and L. Qin, *Trends Biotechnol.*, 2014, 32, 132-139.
- 20 24. R. de la Rica and M. M. Stevens, *Nat. Nanotechnol.*, 2012, 7, 821-824.
- 21 25. R. de la Rica and M. M. Stevens, *Nat. Protoc.*, 2013, 8, 1759-1764.
- 22 26. D. Cecchin, R. de La Rica, R. Bain, M. Finnis, M. Stevens and G. Battaglia, *Nanoscale*, 2014, 6,
23 9559-9562.
- 24 27. X.-M. Nie, R. Huang, C.-X. Dong, L.-J. Tang, R. Gui and J.-H. Jiang, *Biosens. Bioelectron.*, 2014, 58,
25 314-319.
- 26 28. Y. Xianyu, Z. Wang and X. Jiang, *Acs Nano*, 2014, 8, 12741-12747.
- 27 29. K. Simons and E. Ikonen, *Nature*, 1997, 387, 569-572.
- 28 30. S. B. Ficarro, M. L. McClelland, P. T. Stukenberg, D. J. Burke, M. M. Ross, J. Shabanowitz, D. F. Hunt
29 and F. M. White, *Nat. Biotechnol.*, 2002, 20, 301-305.
- 30 31. K. Poelstra, W. W. Bakker, P. A. Klok, J. Kamps, M. J. Hardonk and D. Meijer, *Am. J. Pathol.*, 1997,
31 151, 1163-1169.
- 32 32. B. Nikoobakht and M. A. El-Sayed, *Chem. Mater.*, 2003, 15, 1957-1962.
- 33 33. Z. Guo, X. Fan, L. Xu, X. Lu, C. Gu, Z. Bian, N. Gu, J. Zhang and D. Yang, *Chem. Commun.*, 2011, 47,
34 4180-4182.
- 35 34. Y. Wang, S. Guo, H. Chen and E. Wang, *J. Colloid Interface Sci.*, 2008, 318, 82-87.
- 36 35. C. M. Cheng, A. W. Martinez, J. Gong, C. R. Mace, S. T. Phillips, E. Carrilho, K. A. Mirica and G. M.
37 Whitesides, *Angew. Chem. Int. Ed.*, 2010, 49, 4771-4774.
- 38 36. W. Jiang, Z. Wang, R. C. Beier, H. Jiang, Y. Wu and J. Shen, *Anal. Chem.*, 2013, 85, 1995-1999.
- 39 37. A. Schaap, H. Akhavan and L. Romano, *Clin. Chem.*, 1989, 35, 1863-1864.
- 40 38. A. Hayat, G. Bulbul and S. Andreescu, *Biosens. Bioelectron.*, 2014, 56, 334-339.
- 41 39. A. Hayat and S. Andreescu, *Anal. Chem.*, 2013, 85, 10028-10032.
- 42 40. N. R. Jana, L. Gearheart and C. J. Murphy, *Adv. Mater.*, 2001, 13, 1389.
- 43 41. C. K. Tsung, X. Kou, Q. Shi, J. Zhang, M. H. Yeung, J. Wang and G. D. Stucky, *J. Am. Chem. Soc.*,
44 2006, 128, 5352-5353.
- 45
- 46
- 47
- 48
- 49
- 50
- 51
- 52
- 53
- 54
- 55
- 56
- 57
- 58
- 59
- 60

For TOC only:



1
2
3
4
5
6
7
8
9
10
11
12
13
14
15
16
17
18
19
20
21
22
23
24
25
26
27
28
29
30
31
32
33
34
35
36
37
38
39
40
41
42
43
44
45
46
47
48
49
50
51
52
53
54
55
56
57
58
59
60